Rose Bengal immobilized onto Supported Ionic Liquid-like Phases: Efficient photocatalyst for batch and flow processes

David Valverde,[a] Raul Porcar,[a] Diana Izquierdo,[a] M. Isabel Burguete,[a] Eduardo Garcia-Verdugo*[a] and Santiago V. Luis*[a]

Abstract: The catalytic activity of Rose Bengal immobilized onto supported ionic liquid-like phases has been evaluated as a polymer supported photocatalyst. In these systems, the polymer is designed to play a pivotal role. The polymeric backbone adequately modified with ionic liquid-like moieties (Supported Ionic Liquid-Like Phases, SILLPs) is not just an inert support for the dye but controls the accessibility of reagents/substrates to the active sites and provides specific microenvironments for the reaction. The structure of SILLPs can be fine-tuned to adjust the catalytic efficiency of the RB−SILLP composites achieving systems more active and stable than the related systems in absence of IL-like units.

Introduction

Singlet oxygen is a powerful and versatile reagent that has been applied for a wide range reaction of sequences in order to synthetize molecules with a certain degree of complexity.[1] It can be considered as a green reagent, being generated *in situ* from oxygen through irradiation with visible light of a photosensitizer.[2] The use of singlet oxygen does not produce any waste or residue, other than the photocatalyst, at the end of the process.[3] In this context, different approaches have designed for the immobilization of photosensitizers into a different phase than reactants and products, facilitating its recovery and reuse for further catalytic cycles.[4,5] However, in some cases, this immobilization can lead to a reduction of the photocatalytic efficiency through the quenching of the excited states by the polymeric matrix or by shortening the lifetime of the reactive species. Therefore, an efficient support should provide a suitable environment for the photocatalyst, providing site isolation to prevent dye oligomerization and self-quenching, enhancing quantum yields for singlet oxygen formation and dye photostability.[6-8] The support should also facilitate the accessibility to the immobilized species of the reagents and substrates used in the selected solvents.[9]
Traditionally polymeric supported photocatalysts have been based on hydrophobic matrices, which are hardly compatible with polar or aqueous environments,[10,11] limiting their application to processes performed in organic solvents like chloroform or dichloromethane. To avoid the use of such non-polar VOC solvents, the hydrophilic/hydrophobic balance of the support should be fine-tuned increasing their compatibility with polar solvents like water and alcohols.
Ionic Liquids (ILs) have been evaluated as alternative reaction media for a wide range of catalytic processes,[12-14] and also represent a simple and tunable alternative for the immobilization and stabilization of photosensitizers, opening new avenues for photocatalytic synthetic processes.[15-23] However, processes involving homogenous ILs require the full recovery of the IL-phase and the photosensitizer in a further step, which is not always a simple task. The simplest solution is represented by the use of supported ionic liquids (SILs).[24] In the case of polymers bearing IL-like fragments colantly atttached (Supported Ioinic Liquid-Like Phases: SILLPs) the nature and loading of the IL-like units influence the macroscopic properties of the material,[25] but also plays an important role on the activity and stability of the immobilized catalytic species. Indeed, both the polymer nature and the structural features of the IL-like units can be used to fine-tune their catalytic efficiency.[26] Furthermore, SILPs based on solid-insoluble crosslinked polymers allow their straightforward application for the development of continuous flow processes.[27] In the search of new applications of SILLPs, here we report the synthesis of polymeric materials modified with IL-like units as suitable supports and solid media for photocatalytic processes. The use of supported Rose Bengal, immobilized on a variety of SILLPs, has been evaluated as a photosensitizer for the photooxygenation of furoic acid as a well-established benchmark reaction.

Results and Discussion

IL-like polymeric materials (PILs) were easily prepared by the polymerization of monomers containing imidazolium fragments (Scheme 1).[28-30] Different di-styrenic bisimidazolium monomers were obtained by alkylation of 1-(4-vinylbenzyl)-1H-imidazole with different α,ω-bisbromoalkanes (n= 2, 4 and 6 for **1**-**3** respectively, Scheme SI.1). These crosslinking monomers were co-polymerized with 2-hydroxyethyl methacrylate (**4**, HEMA) using a 4:6 weight ratio, in presence of porogenic agents, leading to a series of monolithic polymers (**5**-**7**). Materials containing different monomer **2** : HEMA ratios were also prepared (**6a-c**). Additionally, the imidazolium monomer **8**, obtained by alkylation of N-butylimidazole with *p*-chloromethyl styrene, was co-polymerized with three different crosslinkers, the divinylic momomer **2**, trimethylolpropane trimethacrylate (**9**) and N,N′-methylene-bis-acrylamide (**10**). Table 1 summarizes

[a] Professor, S. V. Luis and Dr. E. Garcia-Verdugo
Department of Inorganic and Organic Chemistry, Supramolecular and Sustainable Chemistry Group, University Jaume I, Avda Sos Baynat s/n, E-12071-Castellon. Spain. 1
E-mail: luiss@uji.es, cepeda@uji.es

Supporting information for this article is given via a link at the end of the document.

the polymerization mixtures used for preparing all these materials.[31] All of them were obtained in excellent yields (> 95 %) and showed a good compatibility with polar solvents such as water and methanol. Thus, for instance, polymer **11** was able to absorb 45.9 g of water / g of polymer and 24.6 g of MeOH / g of polymer, while polymers **12** and **13**, with higher crosslinking degrees, showed lower absorption capacities (4.8 g water / g and 3.4 g MeOH / g for polymer **12** or 5.7 g of water / g and 3.9 g of MeOH / g for polymer **13**).

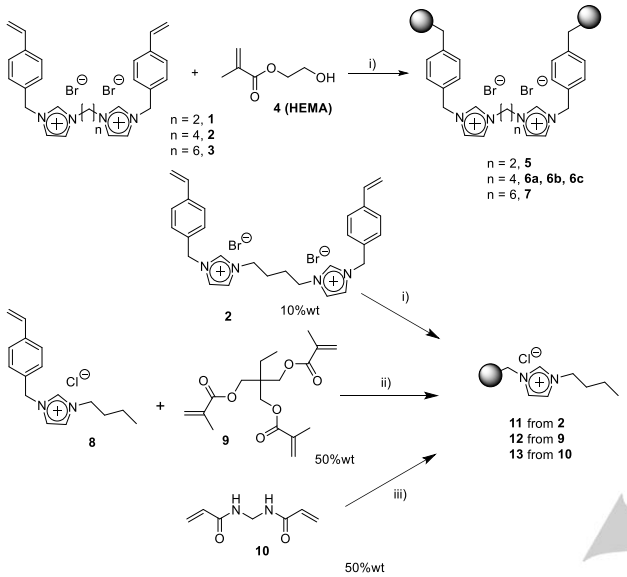

Scheme 1. Synthesis of PILs by polymerization. i) 65 ^{o}C, H_2O, 1% AIBN. ii) 65 ^{o}C, MeOH/H_2O (4:1), 1% AIBN. iii) 70 ^{o}C, MeOH/H_2O (5:1), 1% AIBN.

Table 1. Polymerization mixtures.

Entry	SILLP [a]	IL-monomer (wt/wt)	co-monomer (wt/wt)	Loading mmol/g [b]	% IL [c]
1	**5**	**1** (0.4)	**4** (0.6)	1.24	68.9
2	**6a**	**2** (0.8)	**4** (0.2)	1.58	92.3
3	**6b**	**2** (0.5)	**4** (0.5)	1.38	80.6
4	**6c**	**2** (0.4)	**4** (0.6)	1.25	73.0
5	**7**	**3** (0.4)	**4** (0.6)	1.21	74.1
6	**11**	**8** + **2**(1)	**2** (0.1)	3.17	100
7	**12**	**8** (0.5)	**9** (0.5)	1,27	35.1
8	**13**	**8** (0.5)	**10** (0.5)	2.27	62.0

[a] AIBN 1% by weight of the polymerization mixture, porogen: H_2O/diethylenglycol (1:1 by weight) for **5**, **6** and **7** with a porogen : monomeric mixture ratio of 75:40 by weight. Porogen for **11**: H_2O, porogen for **12**: MeOH H_2O (4:1), porogen for **13**: MeOH H_2O (5:1) with a porogen : momeric mixture ratio of 4.5:1 by weight for **11**, 2.5:1 by weight for **12** and 6.5:1 by weight for **13**. [b] Imidazolium unit loading calculated by elemental analysis. [c] Percentage by weight of the IL-like units calculated as IL (%) = (mmol of imidazolium unit / g polymer) x molecular weight of the imidazolium salt fragment in the corresponding polymer x 10^{-1}.

The immobilization of Rose Bengal (RB) was performed by suspending the polymeric matrices (**5**-**7** and **11**-**13**) in a methanolic solution of RB. Eight different SILLPs, all of them loaded with 3.92 x 10^{-2} mmol RB / g of polymer, were obtained (**15-22**, Scheme 2). The total absence color of the solution indicated the quantitative absorption of RB onto the polymeric matrix. Furthermore, during the polymer washing no color loss was detected and the analysis by UV-Vis at 557 nm of the MeOH used did not show the presence in the washing solution of any trace of leached RB.

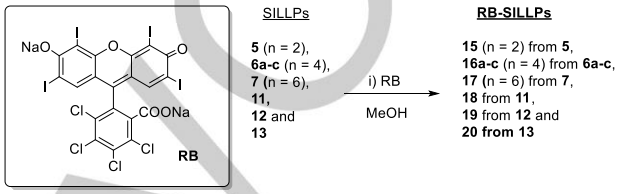

Scheme 2. Immobilisation of RB on SILLPs. i) 1 mL of a 1000 ppm solution of RB in MeOH for each 25 mg of polymer. RB loading 39.36 μmol of RB / g.

In order to evaluate the photocatalytic efficiency of those RB-SILLPs, the photooxygenation of 2-furoic acid **21** to butenolide **22** (5-hydroxy-5H-furan-2-one) was assayed as a benchmark reaction (Scheme 3). A long list of applications of butenolide **22** can be found in the literature, being an important starting substrate for the synthesis of insecticides, prostanoids, alkaloids, etc.[32,33] The oxidation of 2-furoic acid (**21**) to **22** was carried out by irradiating (125 W Hg vapor lamp) a suspension of the corresponding supported photocatalyst in a solution of **21**. The reactions were monitored by UV–vis following the bleaching of the characteristic absorption band of **21** at 247 nm. Both conversions and rate constants were used to analyze the efficiency of the different polymeric photosensitizers.

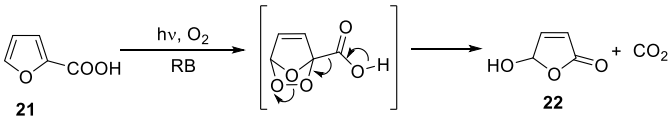

Scheme 3. Photocatalytic benchmark reaction: 50:1 substrate : photocatalyst molar ratio (2% molar), room temperature. Irradiation: 125 W medium pressure Hg vapor lamp for 120 min in open reaction test tubes equilibrated with air. [**21**] = 9.6 mM in MeOH

Under these conditions, all the supported photocatalysts yielded > 90 % conversions after 120 minutes. Essentially, a quantitative selectivity for the transformation of **21** into **22** was observed in all cases. It should be noted that no loss of the characteristic coloration of the Rose Bengal was observed at the end of the reaction in any of the cases studied. Small differences were observed for the kinetic profiles of the tested systems showing, regardless of loading and type of IL-like moieties, similar catalytic efficiencies (Table 2, Fig. SI.1). In the same way, the percentage and type of the crosslinker seems to have little

influence. Noteworthy, faster kinetics were observed for the immobilized RB-SILLPs than for an RB solution and conversions achieved after 120 min were always better than those for the control experiment catalyzed by the disodium salt of RB (95-99% *vs.* 65-70%). The reuse of the photosensitizer **16c** in consecutive reaction cycles was also studied. This RB-SILLP system was very stable, being reused for eight reaction cycles without any decay in its photocatalytic activity (see Fig. SI.2).

Table 2. Photooxydation of 21 by different RB-SILLPs obtained by polymerisation.

Entry	RB-SILLP	Loading mmol/g[a]	% IL[b]	Conv. (%)[c]	$k\ 10^{-4}$ (s^{-1}) [d]
1	**15**	1.24	68.9	99	4.51 ± 0.18
2	**16a**	1.58	92.3	97	3.81 ± 0.06
3	**16b**	1.38	80.6	90	3.29 ± 0.10
4	**16c**	1.25	73.0	98	4.43 ± 0.09
5	**17**	1.21	74.1	99	4.2 ± 0.8
6	**18**	3.17	100	98	5.4 ± 0.3
7	**19**	1,27	35.1	99	5.3 ± 0.3
8	**20**	2.27	62.0	98	5.5 ± 0.19
9	**RB**	-	-	70	3.25 ± 0.11

[a] Imidazolium units loading calculated by elemental analysis. [b] Percentage by weight of the IL-like units calculated as IL (%) = (mmol of imidazolium unit / g polymer) x Molecular weight of the imidazolium salt fragment in the corresponding polymer x 10^{-1}. [c] Conversion for the photo-oxidation of **21**. [d] Rate constants for the photooxidation of **21** calculated as the first-order rate constant for the initial period of the reaction.

Table 3. Effect of the RB loading onto SILLP 6c

Entry	RB-SILLP	µmol of RB/g	$k\ 10^{-4}$ (s^{-1}) [a]	TON [b]	TOF_{50} [c] (h^{-1})
1	**16c**	39.36	4.43 ± 0.09	26	57
2	**23a**	19.84	4.65 ± 0.11	57	114
3	**23b**	0.40	4.95 ± 0.07	289	527
4	**23c**	0.20	1.93 ± 0.012	2867	5213

[a] Rate constant for the photooxidation of **21** calculated as the first-order rate constant for the initial period of the reaction. [b] TON calculated at 30 min. [c] TOF calculated at 50% of conversion.

Encouraged by these results, the effect of different variables was evaluated in order to optimize the efficiency of the immobilized system. In this way, the influence of the RB loading on the SILLP was firstly examined. Variable amounts of RB were absorbed onto the polymer **6c** (39.36 to 0.20 µmol of RB / g of SILLP, polymers **16c** and **23a-b**). Results obtained are summarized in Table 3 and Fig. SI.3. A complete conversion of **21** was observed after 60 min of reaction for the catalyst with the higher RB loading (**16c**), while an irradiation time of 180 minutes was required for the photocatalyst with the lowest RB-loading (**23c**). The photocatalysts with intermediate loadings (**23a** and **23b**) showed similar profiles of yield *vs* time (Fig SI.3) than **16c**, albeit their RB loadings were 2 and 10 times lower, respectively. Thus, the highest TON and TOF_{50} values were obtained for **23c**, a polymer with a very low RB loading (0.2 µmol/g) with TON = 2867 (30 min) and TOF_{50} = 5213 h^{-1}. These results suggest that for the polymeric photosensitizer **16c** (having the highest loading, 39.36 µmol of RB/g of SILLP) RB groups located near the surface of the polymer can act as a filter, absorbing the incident radiation and preventing it from reaching the dye groups located in more hindered sites ("screen effect"). This effect decreases upon the reduction of the RB loading, increasing the catalytic efficiency per dye unit. All the systems presented so far are based in SILLPs obtained by copolymerization of the corresponding IL-monomers (Scheme 1). In order to stablish the effect of the polymer matrix on the behavior of the photosensitizers, a new series of gel type SILLPs were synthesized (Scheme 4) by grafting IL-like units onto already preformed polystyrene-divinylbenzene polymeric matrices (PS-DVB, Merrifield gel-type resins). Three different SILLPs (**25a-c**) were synthetized by modification of PS-DVB resins with different loadings (1.1, 2.1 and 4.1 meq Cl / g, **24a-c**, 1% DVB, gel-type, 200-400 mesh).

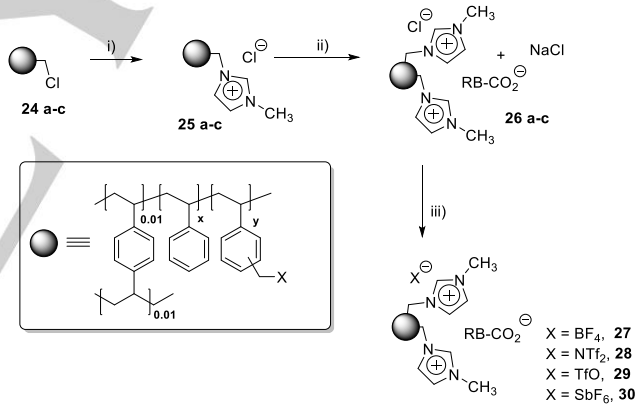

Scheme 4. Synthesis of gel-type SILLPs and the corresponding RB photocatalysts i) methylimidazole in DMF, 80 °C, 14 hours. ii) 1 mL of a 1000 ppm solution of RB in MeOH for each 25 mg of polymer. RB loading 39.36 µmol of RB / g. iii) anion metathesis with the corresponding salt in MeOH.

The modification with methylimidazole took place quantitatively with a significant change on the resin polarity. SILLPs **25a-c**, although based on a PS-DVB hydrophobic polymeric backbone, showed a significant swelling in a polar solvent like MeOH, with swellings of 40%, 59% and 84% (percentage of diameter increase in methanol) for **25a**, **25b** and **25c** respectively. RB was quantitatively absorbed on polymers **25a-c** and the resulting RB-SILLPs (**26a-c**) were assayed for the model photooxidation of furoic acid **21**. Results obtained are summarized in Table 4 and Fig SI.4. The different kinetic profiles observed for these systems suggest that the amount of IL-like units can be used to fine-tune the catalytic behavior of the RB-SILLPs. For the

polymers with a low loading of IL-like moieties (**26a**), the limited swelling in MeOH can provide a less effective diffusion of reagents and oxygen through the polymer beads. In this regard, a good diffusion is essential since $^1O_2$ is a short lived species that might be quenched by the protic solvent before meeting the substrate. Besides, a lower swelling can also produce local photocatalyst aggregates (higher local concentration), which would decrease the photochemical activity.

Table 4. Effect of the amount of IL-like units on the SILLPs.

Entry	Cat	Loading[a] (mmol/g)	% IL[b]	k 10^{-4} (s^{-1}) [c]
1	**26a**	0.89	23	2.99 ± 0.03
2	**26b**	1.92	45	7.90 ± 0.40
3	**26c**	2.99	70	5.13 ± 0.08

[a] Imidazolium units loading calculated by elemental analysis. [b] Percentage by weight of the IL-like units calculated as IL (%) = (mmol of imidazolium unit / g polymer) x Molecular weight of the imidazolium salt fragment in the corresponding polymer x 10^{-1}. [c] Rate constants for the photooxidation of **21** calculated as the first-order rate constant for the initial period of the reaction.

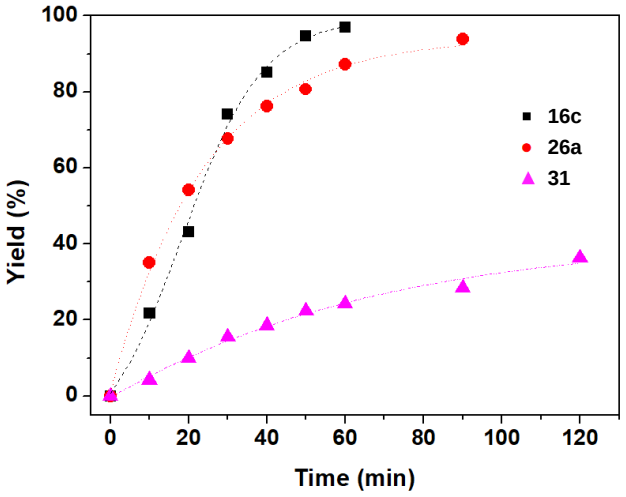

Figure 1. Comparison of yield *vs* time profiles obtained for the oxidation 2-furoic acid with singlet oxygen ($^1O_2$) in the presence of RB-SILLPs **16c** and **26a** and in the presence of commercial RB-PS-DVB **31**. 50:1 substrate : photocatalyst molar ratio (2% molar), room temperature. Irradiation: 125W medium pressure Hg vapor lamp for 120 min in open reaction test tubes equilibrated with air. [**21**] = 9.6 mM in MeOH. Squares: **16c**. Dots: **26a**. Triangles: **31** (Necker´s catalyst). Initial reaction rates: 6.19 ± 0.12 x 10^{-4} (s^{-1}) for **16c**; 6.40 ± 0.14 x 10^{-4} (s^{-1}) for **26a** and 0.82 ± 0.02 x 10^{-4} (s^{-1}) for **31**.

The photocatalytic activity was clearly improved by the enhanced swelling in MeOH for **26b**. However, the further increase in swelling for **26c** is accompanied by some decrease in activity. The much larger diameter of the polymeric beads for **26c** when swollen, can hamper the efficient radiation absorption by the RB units at the core of the particles. Accordingly, a compromise between the loadings of both the photocatalyst and the IL-like units must be reached to achieve the best catalytic performance.

These results suggest that the IL-like units in the support allow a fine-tuning of the photocatalytic efficiency of RB. This is highlighted in Fig. 1, which shows a comparison of the RB-SILLPs **16c** and **26a** with the commercially available RB grafted onto PS-DVB (1% crosslinking, 0.1 mmol RB / g, 200-400 mesh, **31**). RB immobilized on polymers containing IL-like units (SILLPs) was clearly more active systems that when supported on a polymer lacking such units, with the initial reaction rate being *ca*. 7.5 times higher for RB-SILLPs.

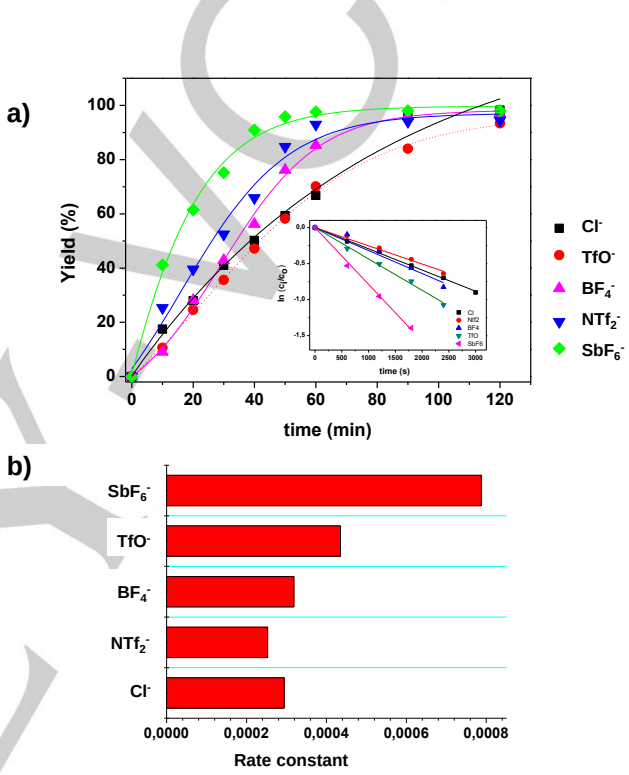

Figure 2. a) Yield *vs* time profiles obtained for RB-SILLPs derived from **26a** by anion metathesis (**27a-30a**) for the oxidation 2-furoic acid with singlet oxygen ($^1O_2$). Inset: $\ln(C_i/C_0)$=kt for the initial period of the reaction, where C_i and C_0 are the concentrations of **21** at a certain time (t) and at t = 0, respectively. Conditions: 50:1 substrate : photocatalyst molar ratio (2% molar), room temperature. Irradiation: 125W medium pressure Hg vapor lamp for 120 min in open reaction test tubes equilibrated with air. [**21**] = 9.6 mM in MeOH. b) Effect of the IL-like moieties counteranion on the rate constants.

The nature of the anion can also be used to tune the properties of catalytic units immobilized onto SILs.[34-36] Therefore, the effect of the anion was evaluated by exchanging the Cl^- anion of the RB-SILLP **26a** by BF_4^-, NTf_2^-, TfO^- and SbF_6^- (RB-SILLPs **27a-30a**, Scheme 4). ATR-FTIR and Raman spectroscopy were used to follow the corresponding anion exchange,[25] while diffuse reflectance UV-vis spectroscopy was used to analyze the presence of Rose Bengal. It has been reported that RB grafted onto Merrifield resins display two high intensity absorption bands located between 571 and 560 nm.[37] The presence of a shoulder at shorter wavelengths (*ca*. 530 nm) has been associated to the formation dimers or aggregates in homogeneous and supported

RB esters.[38,39] RB-SILLPs displayed two broad bands at 566±3 and 523±4 nm, affected in position and intensity by the counteranion present (Fig. SI.5 and Table SI.1) along with a small shoulder below 500 nm. These changes highlight the very different environment for the dye present in RB-SILLPs and that is also affected by the nature of IL-like fragments counteranion. Independently of the anion present, most photosensitizers showed a similar activity (Fig. 2). Only **30**a bearing SbF_6^- as the anion, showed an increased reactivity in comparison with the photosensitizers containing Cl^-, TfO^-, NTf_2^- and BF_4^-, which can be related to the low coordinating ability of this anion facilitating a tighter interaction of RB with the IL-fragments.

All the above reactions were assayed with high-pressure Hg lamps, which can be considered as the standard light source for UV photochemical reactions. However, for this type of light source, there is some mismatch between the light emitted and the absorption frequency of the target molecular dye, which can lead to reduction in efficiency, photocatalyst deactivation, degradation of products and less selective processes. Therefore, the use of using simple LEDs, instead of the Hg lamp, was also evaluated. UV-LEDs allow energy efficient, reliable, and simple generation of almost monochromatic near-UV light, and allow a straightforward building of cheap photochemical reactors. Figure SI.6 shows the comparison of the results obtained from RB in solution as well as with the RB-SILLP **27a**, using the Hg lamp and green UV-LEDs, for the photooxidation of **21**. Comparable results were obtained, especially regarding the initial rates, although the Hg lamp, with a higher power, achieved slightly higher final yields.

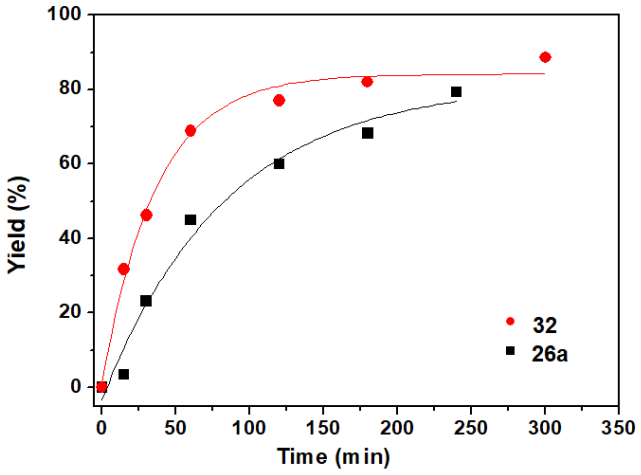

Figure 3. Yield *vs* time profiles obtained for the oxidation 2-furoic acid with singlet oxygen ($^1O_2$). Conditions: 50:1 substrate : photocatalyst molar ratio (2% molar), room temperature. Irradiation: Blue LED for 300 mim in open reaction test tubes equilibrated with air. [**21**] = 9.6 mM in MeOH. Squares: **26a**. Dots: **32** (QDs-RB-SILLP). Initial reaction rates: 1.32 ± 0.09 x 10^{-4} (s^{-1}) for **26a**; 4.05 ± 0.08 x 10^{-4} (s^{-1}) for **32**.

Besides, the use of LEDs can open new avenues in the search for more efficient photocatalytic processes. This is illustrated by the combination of RB-SILLPs with a semiconductor quantum dot (QD, *i.e.* CdSe), acting as a 'light antenna' to capture energy at a wavelength not usable directly by the photosensitizer.[40,41] Thus, a QDs-SILLP (**31**) composite was easily obtained by exposing SILLP **25a** to solution of core–shell CdSe/ZnS QDs (50 µg/mL in toluene). UV-Vis data indicated a quantitative immobilization of the QDs in the SILLP. Then, RB was supported on the QDs-SILLP, affording the QDs-RB-SILLP composite (**32**) with a loading of 60 µg of QDs / g and 39.36 µmol of RB / g of composite. As seen in Fig. 3, the use of the composite **32** allowed the photooxidation to occur efficiently when irradiating with blue UV-LEDs. Thus, at 15 minutes a 32% conversion was obtained for the QDs-RB-SILLP **32**, while only a 5 % yield was achieved with the related RB-SILLP **26a**. This suggests the existence of an effective Förster's Resonance Energy Transfer (FRET) process leading to the indirect excitation of the RB moiety when exciting the QD nanoparticle. The overlapping between the emission of QDs and the absorption of RB at the SILLP leads to population of the RB triplet state and concomitantly to the efficient generation of singlet oxygen. Nevertheless, the process was less efficient that when irradiating directly **26a** with green UV-LEDs (Fig. 3) even if the initial rates were comparable.

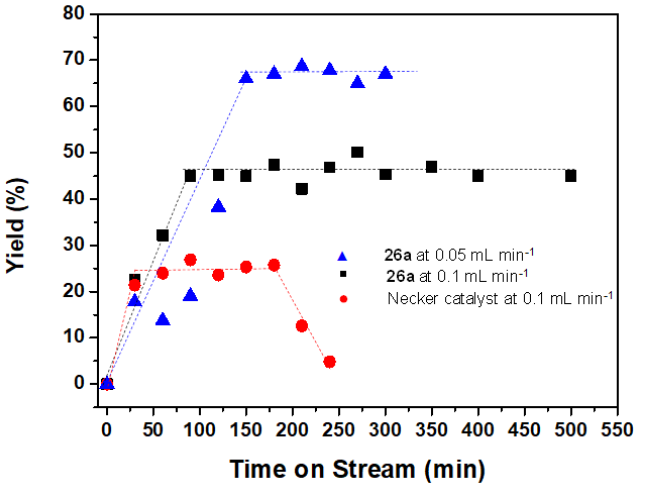

Figure 4. Yield *vs* time on stream obtained for the photooxidation of **21**. Dots: Necker catalyst at 0.1 mL min^{-1}. Squares: **26a** at 0.1 mL min^{-1}. Triangles: **26a** at 0.05 mL min^{-1}.

Continuous flow processes can help to increase the sustainability of photocatalytic reactions as they present some distinct advantages such as the easy separation of products and the continuous reutilization of the photocatalyst in consecutive cycles, avoiding downtime, and the consequent loss of productivity.[42] Fig. SI.7 shows a schematic representation of the continuous flow reactor used to perform the photooxidation of furoic acid. The system consists in a HPLC pump that feeds the substrate to the reactor, which is a fluid bed reactor loaded with RB-SILLP. A Hg lamp was used as the light source. The behavior of **26a** was compared with that of the commercially available Necker catalyst (RB-PS-DVB).[10] Figure 4 summarizes the results obtained. Using an initial flow rate of 0.1 mL min^{-1}, the commercial catalyst provided a yield of *ca.* 25 %, which was lower than the one achieved with **26a** (*ca.* 45% yield).

Furthermore, the commercial catalyst showed a strong deactivation after 200 min on continuous use, while the performance of the RB-SILLP remained constant during at least 8 hours. The yield with **26a** could be further improved until *ca.* 70% by increasing the residence time through reducing the flow rate to 0.05 mL min^{-1}. These results suggest that the continuous flow photochemical generation of singlet oxygen can be achieved by the simple immobilization RB onto SILLPs providing a scalable, selective and high-yielding platform, where the oxidation proceeds using only light, air and catalytic amounts of supported RB.

Conclusions

Rose Bengal immobilized onto SILs prepared by direct copolymerization of imidazolium monomers or by grafting imidazolium units on already performed polymers efficiently promotes the photooxidation of furoic acid by generation of singlet oxygen. The supported photocatalysts are equally active under irradiation using an Hg lamp or, alternatively, under UV-LEDs irradiation. The chemical and structural parameters of the SILLPs can be easily fine-tuned to optimize the catalytic efficiency of the RB-SILLPs. Adjusting the IL-like units loading as well as the nature of the IL-counteranion has allowed obtaining supported catalysts that are significantly more active than related systems lacking the IL-like units, including commercially available RB-PS-DVB systems. Furthermore, the presence of these IL-like units facilitates the immobilization and stabilization of QDs working as light antennas to increase the light harvesting capacity at wavelengths not corresponding to the optimal absorption of RB. Optimized RB-SILLPs showed a remarkable stability and this has been used for developing an efficient continuous mini-flow photocatalytic process implemented for the photooxidation of **21**, which demonstrated to be a more active and stable system than the related one using the commercial polymer where the photosensitizer is grafted to a PS-DVB backbone in the absence of IL-like units. These results open a new avenue for the combination of advanced materials based on polymeric ionic liquids with organic photo-dyes to develop more efficient and easier to use photocatalytic systems.

Experimental Section

Materials: All the reagents and solvents used were commercially available. 4-vinylbenzyl chloride (p-chloromethylstyrene, 90%, Aldrich) was purified over a column of basic aluminium oxide. 2,2′ -Azobis(2-methylpropionitrile) used as free radical initiator (AIBN, >98%, Aldrich), N,N-dimethylformamide (DMF, 99.5%, Scharlau), 1-methylimidazole (99%, Aldrich), 1-butylimidazole (98%, Aldrich), 1-decyl-2-methylimidazole (97% Aldrich), trimethylolpropane trimethacrylate (technical grade, TMPTMA Aldrich), N,N′ -methylenebis(acrylamide) (99% Aldrich), 4,5,6,7-tetrachloro-2′ ,4′ ,5′ ,7′ -tetraiodofluorescein disodium salt, Acid Red 94, Rose Bengal B sodium salt (Rose Bengal sodium salt, 95%, Aldrich), polystyrene-bound Rose Bengal B (200-400 mesh, ~0.1 mmol / g, Aldrich), chloromethylated stryene/divinylbenzene copolymer resins (Merrifield peptide resin, 200-400 mesh, 1.2, 2.1 or 4.3 mmol / g Cl^- loading, 2 % cross-linked), methanol (MeOH, 99.9%, Scharlau), bis(trifluoromethane) sulfonimide lithium salt ($LiNTf_2$, 99%, Aldrich), acetone HPLC (99.9%, Scharlau) and other salts and solvents were used as received.

General characterization protocols: FT-IR spectra were obtained using a spectrometer (JASCO FT/IR-6200) equipped with an ATR (MIRacle single-reflection ATR diamond/ZnSe) accessory at 4 cm^{-1} resolution (4000-600 cm^{-1} spectral range). Raman spectra were obtained with a NRS-3100 (Jasco) dispersive Raman spectrometer equipped with an optical microscope and an air-cooled CCD detector (-65 ºC) using the following conditions: 785 nm laser with a single monochromator, 600 l/mm grating, 0.2 mm slit, 12.75 cm^{-1} resolution; with a center wavenumber of 1200 cm^{-1}, a laser power of 90.1 mW and 10 accumulations of 5 s. Elemental analyses were obtained with a CHN Euro EA 3000 instrument. ^{1}H-NMR experiments were carried out using a Varian INOVA 500 (^{1}H-NMR, 500 MHz) spectrometer. Chemical shifts are given in delta (δ) values relative to TMS and the coupling constants (*J*) in Hertz (Hz). UV-Vis spectroscopy measurements were performed in a Shimadzu UV2450 spectrophotometer (diffuse reflectance mode for polymers) using an integrated sphere accessory and a light wavelength range between 200 and 800 nm.

Synthetic protocols: Monomers **1**-**3** and **8** were obtained as shown in Scheme SI.1 according to methods already reported in the literature.[43]

Synthesis of 1-(4-vinylbenzyl)-1H-imidazole. $NaHCO_3$ (5.25 g, 62.4 mmol, 1.25 eq) was added to a mixture of imidazole (13.61 g, 199 mmol, 4 eq) in CH_3CN, then 1-(chloromethyl)-4-vinylbenzene (7.1 mL, 49.8 mmol, 1 eq) was added dropwise at RT. After the addition, the reaction mixture was heated to 50 ºC and stirred for 20 h. The solvent was removed in vacuum, and the remaining solution was extracted with diethyl ether. The organic phase was washed with 2 M HCl (final pH = 4-5) 4 M NaOH was then added to the resulting aqueous phase until pH = 7-8 (cloudy solution), and this solution was extracted with diethyl ether. The obtained organic phase was dried over Na_2SO_4 and the solvent was removed in vacuum to afford the desired 1-(4-vinylbenzyl)-1H-imidazole (6.55 g, 71 % yield).

FT-IR (cm^{-1}): 3005; 1570; 1505; 1408; 1320; 1285; 1231; 1017; 825; 745; 622. Raman (cm^{-1}): 3059; 1622; 1571; 1409; 1347; 1205; 1182; 1075; 831; 639. ^{1}H NMR (CD_3OD, 500 MHz), δ (ppm): 5.08 (s, 2H), 5.27 (d, *J* = 10.9 Hz, 1H), 5.75, (d, *J* = 17.9 Hz, 1H), 6.66-6.71 (m, 1H), 6.88 (d, *J* =17.7 Hz, 2H), 7.08 (d, *J* = 9.5 Hz, 2H), 7.36 (d, *J* = 8.1 Hz, 2H), 7.53 (s, 1H). ^{13}C NMR (CD_3OD, 300 MHz) δ (ppm) 49.9, 115.2, 120.9, 127.1, 128.4, 129.4, 136.8, 137.3, 138.1. ESI/MS (m/z). [M+H] = 185.2.

General procedure for the synthesis of ionic monomers 1-3. 1-(4-vinylbenzyl)-1H-imidazole (4.2 mmol), the appropriate dibromo-alkyl spacer (2 mmol), and CH_3CN (10 mL) were loaded into a 25 mL two - necked flask. The mixture was heated to 80 °C for 24 h. The reaction mixture was cooled down to RT and transferred to a 100 mL round - bottomed flask. The product was precipitated with Et_2O (50 mL) and sonicated for 10 min, and the white solid was then left to settle. The liquid phase was removed carefully, and the washing procedure was repeated twice with Et_2O (2 × 50 mL). Finally, the white solid product was dried under vacuum overnight.

3,3′ - (Ethane - 1,2 - diyl)bis(1 - (4 - vinylbenzyl) - 1 H - imidazol - 3 - ium) chloride (**1**). Obtained as a white solid in 60% yield using the former standard procedure.

FT-IR (cm^{-1}): 3053; 1558; 1416; 1341; 1156; 988; 908; 857; 795; 623. Raman (cm^{-1}): 1620, 1601, 1414, 1316, 1195, 1174, 1016, 828, 629, 291. ^{1}H-NMR (CD_3OD, 500 MHz) δ (ppm) 4.74 (s, 4H), 5.28 (d, *J* = 10.9 Hz, 2H), 5.41 (s, 4H), 5.84 (d, *J* = 17.7 Hz, 2H), 6.70-6.76 (m, 2H), 7.35 (d, *J* = 18.1 Hz, 4H), 7.49 (d, *J* = 8.1 Hz, 4H), 7.72 (d, *J* = 7.9 Hz, 2H), 7.82 (d, *J* = 7.9 Hz, 2H), 9.32 (s, 2H). ^{13}C RMN (CD_3OD, 300 MHz) δ (ppm), 35.5,

53.0, 114.5, 122.9, 123.3, 127.0, 129.1, 133.5, 136.0, 139.1. ESI/MS (m/z) [M^{2+}-2Br/2] = 198.2.

3,3′ - (Butane - 1,4 - diyl)bis(1 - (4 - vinylbenzyl) - 1 H - imidazol - 3 - ium) chloride (2). Obtained as a white solid with 83% yield using the former standard procedure.

FT-IR (cm^{-1}): 3143, 1561, 1459, 1156, 1009, 929, 860, 744, 627. Raman (cm^{-1}): 1620, 1598, 1408, 1317, 1195, 1176, 1011, 825, 627, 315.

^{1}H-NMR (CD_3OD, 500 MHz) δ (ppm) 1.95 (s, 4H), 4.30 (s, 4H), 5.28 (d, *J* = 10.2 Hz, 2H), 5.30 (s, 4H), 5.82, (d, *J* =15.3 Hz, 2H), 6.70-6.75 (m, 2H), 7.39 (d, *J* = 16.3 Hz, 4H), 7.48 (d, *J* = 7.6, 4H), 7.62 (d, *J* = 7.6 Hz, 2H), 7.68 (d, *J* = 7.6 Hz, 2H), 9.28 (s, 2H). ^{13}C RMN (CD_3OD, 300 MHz) δ (ppm) 26.8, 30.1, 48.9, 52.4, 116.0, 123.3, 123.5, 127.4, 129.4, 134.9, 136.6, 138.3. ESI/MS (m/z) [M^{2+}-2Br/2] = 212.3.

3,3′ - (Hexane - 1,6 - diyl)bis(1 - (4 - vinylbenzyl) - 1 H - imidazol - 3 - ium) chloride (3). Obtained as a white solid with 78% yield using the former standard procedure.

FT-IR (cm^{-1}): 3053, 1557, 1451, 1153, 922, 829, 740, 639. Raman (cm^{-1}): 1615, 1598, 1398, 1301, 1192, 1013, 818, 629, 599, 323. ^{1}H-NMR (CD_3OD, 500 MHz) δ (ppm) 1.41 (s, 4H), 1.92 (s, 4H), 4.24 (s, 4H), 5.28 (d, *J* = 10.1 Hz, 2H), 5.42 (s, 4H), 5.79 (d, *J* = 15.6 Hz, 2H), 6.71-6.75 (m, 2H), 7, 41 (d, *J* = 17.0 Hz, 4H), 7.50 (d, *J* = 8.2, 4H), 7.63 (d, *J* = 7.9 Hz, 2H), 7.68 (d, *J* =7.8 Hz, 2H), 9.18 (s, 2H). ^{13}C RMN (CD_3OD, 500 MHz) δ (ppm) 25.8, 48.5, 112.1, 119.3, 119.6, 123.4, 123.5, 131.1, 132.7, 132.9, 136.8, 138.3. ESI/MS (m/z) [M^{2+}-2Br/2] = 226.3.

Synthesis of 1-[(4-Ethenylphenyl)methyl]-3-butyl-imidazolium chloride (8): 1-butylimidazole (125 mmol) was dissolved in CH_3CN (30 mL) in a 100 mL round-bottom flask equipped with a stir bar. 4-Chloromethylstyrene (19.5 mL, 139 mmol) was then added, and the reaction was heated at 50 °C while stirring overnight. The reaction was stopped after this time, and the reaction mixture was poured into Et_2O (250 mL). The ionic product precipitated, and the mixture was placed in a freezer for several hours. The Et_2O phase was decanted and the resulting solid dried under vacuum lines at 40 °C overnight. Yield = 53.73 g, 82%. Characterization data were consistent with published values.[43]

General procedure for the preparation of the polymers 5-7 and 11-13 by bulk polymerization. The polymerization mixture was prepared using the corresponding composition of the monomeric mixture as shown in Table 1 and different weight percentages (wt%) of the solvent mixture used as the porogen an reported in the same table. The initiator, AIBN, was 1% of the mass of the monomers. The mixture was vortexed, sonicated and degassed until homogenous, then poured into a test tube and placed in a hot bath at 70 °C for 24 hours. The resulting polymers were washed in a Soxhlet (MeOH) to remove the unreacted starting materials. The polymerization took place in all the cases with > 95% yield.

Polymer 5: FT-IR (cm^{-1}): 2943, 1721, 1563, 1456, 1392, 1271, 1157, 1078, 1025, 848, 757. Raman (cm^{-1}): 1603, 1440, 1267, 1179, 1015, 956, 820, 593, 306. CHN analysis: %N (found): 3.4%, loading 1.24 mmol IL-like units / g of polymer. %N (expected): 3.73% for 1.33 mmol IL-like units / g of polymer.

Polymer 6a: FT-IR (cm^{-1}): 2945, 1720, 1564, 1457, 1389, 1155, 845, 760, 623. Raman (cm^{-1}): 1603, 1440, 1179, 1014, 957, 821, 631, 594, 306. CHN analysis: %N (found): 4.4%, loading 1.58 mmol IL-like units / g of polymer. %N (expected): 4.54% for 1.62 mmol IL-like units / g of polymer.

Polymer 6b: CHN analysis: %N (found): 3.9%, loading 1.38 mmol IL-like units / g of polymer. %N (expected): 3.90% for 1.4 mmol IL-like units / g of polymer.

Polymer 6c: CHN analysis: %N (found): 3.5%, loading 1.25 mmol IL-like units / g of polymer. %N (expected): 3.59% for 1.28 mmol IL-like units / g of polymer.

Polymer 7: FT-IR (cm^{-1}): 2946, 1721, 1562, 1455, 1392, 1273, 1157, 1076, 1022, 847, 757. Raman (cm^{-1}): 1604, 1440, 1411, 1322, 1179, 1015, 822, 632, 595, 307. CHN analysis: %N (found): 3.4%, loading 1.21 mmol IL-like units / g of polymer. %N (expected): 3.47% for 1.24 mmol IL-like units / g of polymer.

Polymer 11. FT-IR (cm^{-1}): 3382, 3133, 3058, 2959, 2928, 2870, 1630, 1613, 1560, 1513, 1453, 1425, 1359, 1326, 1155, 1117, 1020, 850, 825. CHN analysis: %N (found): 8.9%, loading 3.17 mmol IL-like units / g of polymer. %N (expected): 9,10% for 3.25 mmol IL-like units / g of polymer.

Polymer 12. FT-IR (cm^{-1}): 3375, 2959, 2940, 2877, 1720, 1634, 1560, 1459, 1387, 1266, 1148, 1013, 973, 817, 756. CHN analysis: %N (found): 3.6%, loading 1.27 mmol IL-like units / g of polymer. %N (expected): 3.64% for 1.30 mmol IL-like units / g of polymer.

Polymer 13. FT-IR (cm^{-1}): 3272, 3057, 2959, 2933, 2872, 1644, 1515, 1381, 1213, 1113, 816. CHN analysis: %N (found): 6.4%, loading 2.27 mmol IL-like units / g of polymer. %N (expected): 6.44% for 2.3 mmol IL-like units / g of polymer.

Standard procedure for the preparation of polymers 15-20. 500 mg of the corresponding SILLP (**5-7** and **11-13**) was suspended in 20 mL of a solution of RB (1000 ppm in MeOH) and left under stirring for 24 h. Then the polymer was filtered, washed with MeOH and dried in a vacuum oven at 45 °C. The absorption for RB at 557 nm was measured in the mother liquor and in the washing liquid. In all cases the absorption corresponded with a quantitative uptake. RB loading: $3.98.10^{-3}$ mmol of RB / g polymer.

General synthesis of polymers 25a-c. The synthesis was performed as already reported.[44] A Merrifield resin (10 g, **24a-c**) was introduced in a round-bottomed flask (250 mL) then, the alkylimidazole (6 eq.) was dissolved in DMF (100 mL) and introduced in the flask and the suspension was refluxed for 14 hours. The NBP test was negative at the end of this period confirming full conversion of chloromethyl groups.[45] The reaction was then filtered and the polymer was washed with DMF, DMF : H_2O (1:1), THF and CH_2Cl_2 and dried in a vacuum oven at 60 ºC.

Polymer 25a: FT-IR (cm^{-1}): 3419, 3141, 3060, 2922, 2848, 1567, 1616, 1510, 1449, 1332, 1159, 1022, 823, 761, 706, 661, 619. Raman (cm^{-1}): 1612, 1579, 1450, 1413, 1385, 1331, 1188, 1160, 1091, 1022, 1001, 831, 765, 716, 664, 642, 620, 411, 332. CHN analysis: %N (found): 2.5%, loading 0.89 mmol IL-like units / g of polymer. %N (expected): 2.6% for 0.93 mmol IL-like units / g of polymer.

Polymer 25b: FT-IR (cm^{-1}): 3023, 2924, 1561, 1450, 1160, 824, 762, 703, 661.4, 619, 548. Raman (cm^{-1}): 1605, 1406, 1325, 1181, 1015, 995, 824, 636, 614. CHN analysis: %N (found): 5.4%, loading 1.92 mmol IL-like units / g of polymer. %N (expected): 5.9% for 2.1 mmol IL-like units / g of polymer.

Polymer 25c: FT-IR (cm^{-1}): 3931, 3891, 3830, 3738, 3386, 3147, 3086, 2925, 1644, 1566, 1515, 1451, 1334, 1159, 824, 761, 706, 616. Raman (cm^{-1}): 1615, 1455, 1415, 1387, 1332, 1192, 1092, 1024, 1004, 836, 769, 669, 646, 624, 414, 358, 270, 149. CHN analysis: %N (found): 10.6%, loading 3.79 mmol IL-like units / g of polymer. %N (expected): 10.44% for 3.73 mmol IL-like units / g of polymer.

General procedure for the preparation of polymers 26a-c. 500 mg of the corresponding SILLP (**25a-c**) was suspended in 20 mL of a solution of RB (1000 ppm in MeOH) and left under stirring for 24 h. Then the polymer was filtered, washed with MeOH and dried in a vacuum oven at 45 °C. The absorption for RB at 557 nm was measured in the mother liquors and in the washing liquid. In all cases the absorption corresponded with a quantitative uptake. RB loading $3.98.10^{-3}$ mmol of RB / g polymer.

General procedure for the preparation of polymers 27-30. 100 mg of the corresponding SILLP (**26a**) was suspended in 12 mL of a MeOH : H_2O mixture (10:1 v/v) containing an excess of the corresponding YX salt and left under stirring for 24 h. Then the polymer was filtered, washed with MeOH and dried in a vacuum oven at 45 °C.

Polymer 27: YX = $NaBF_4$. FT-IR (cm^{-1}): 3026, 2922, 1596, 1496, 1448, 1350, 1194, 1057, 756, 700, 613. Raman (cm^{-1}): 1592, 1439, 1317, 1174, 1145, 1020, 990, 784, 610, 397. CHN analysis: %N (found): 2.2%, loading 0.77 mmol IL-like units / g of polymer. %N (expected): 2.25% for 0.80 mmol IL-like units / g of polymer.

Polymer 28. YX = $LiNTf_2$. FT-IR (cm^{-1}): 3026, 2922, 1596, 1496, 1448, 1350, 1194, 1057, 756, 700, 613. Raman (cm^{-1}): 1591, 1438 1317, 1172, 1144, 1019, 990, 782, 730, 610, 395. CHN analysis: %N (found): 2.5%,

loading 0.60 mmol IL-like units / g of polymer. %N (expected): 2.92% for 0.69 mmol IL-like units / g of polymer.

Polymer 29. YX = KTfO. FT-IR (cm^{-1}): 3026, 2922, 1596, 1452, 1267, 1159, 1026, 757, 700, 632, 544. Raman (cm^{-1}): 1592, 1483, 1174, 1145, 1020, 991, 783, 747, 611. CHN analysis: %N (found): 2.04%, loading 0.73 mmol IL-like units / g of polymer. %N (expected): 2.14% for 0.76 mmol IL-like units / g of polymer.

Polymer 30. YX = $KSbF_6$. FT-IR (cm^{-1}): 3026, 2922, 1596, 1487, 1450, 1159, 757, 700, 653, 626, 545. Raman (cm^{-1}): 1591, 1439, 1317, 1174, 1145, 1020, 991, 784, 611, 399. CHN analysis: %N (found): 2.0%, loading 0.70 mmol IL-like units / g of polymer. %N (expected): 2.01% for 0.72 mmol IL-like units / g of polymer.

Synthesis of polymer 32: To a suspension of SILLP **25a** (250 mg) in DMF (5 mL), 1.5 mL of a QDs solution in toluene (CdSe/ZnS, 510nm, 50 µg / mL) was added and the mixture left under stirring (300 rpm) and protected from the light during 24 h. Then, the polymer was filtered, washed with DMF : H_2O (1:1), H_2O, CH_2Cl_2 and MeOH (5x5 mL) and dried under vacuum at 45 °C. QDs loading: 0.3 mg QDs / g polymer.

100 mg of this resin (**31**) were suspended in a 1000 ppm solution of RB in MeOH (4 mL) and left under stirring (300 rpm) and protected from the light for 24 h. Afterwards, the polymer was filtered, washed with DMF : H_2O (1:1), H_2O, CH_2Cl_2 and MeOH (5x5 mL) and vacuum dried at 45 °C. RB loading: $3.98.10^{-3}$ mmol of RB / g polymer.

Standard protocol for the photooxidation of 2-furoic acid (21) to 5-hydroxy-5H-furan-2-one. The corresponding photosensitizer was added to 10 mL of a methanolic solution of 2-furoic acid (9.6 mM) in a test tube. The heterogeneous mixture was kept under stirring and in equilibrium with air. These test tubes were placed at 2 cm of a 0.1 M aqueous solution of $FeCl_3$ used as a filter for wavelengths lower than 450 nm and irradiated with a 125-W medium-pressure Hg vapor lamp for at least 6 h. The same experimental conditions were used in the dark in order to evaluate a possible adsorption of the substrate into the polymer. Moreover, the following control experiments were carried out: (a) irradiation in the absence of polymer and (b) irradiation of 2-furoic acid with free Rose Bengal in solution (5 µM) as the photosensitizer. The decreasing absorbance of 2-furoic acid was monitored by means of UV–vis spectroscopy at 246 nm. For each measurement, 80 µL aliquots were removed from the reaction mixture and diluted in 25 mL of the appropriate solvent. The initial rate constants for each oxidation reaction were calculated as first-order rate constants (*k*) as reported in the literature.[41] At the end of the irradiation period the solutions were filtered, concentrated, and the product obtained in these irradiations was identified as pure butenolide **22** by ^{1}H-NMR, ^{13}C-NMR and MS. The ability of the photosensitizer to generate singlet oxygen was demonstrated using the RB-SILLPs as photocatalysts for the chemical oxidation of 9,10-diphenylanthracene (DPA) to its endocyclic endoperoxide.[46,47]

Continuous flow photooxidation of 21. A solution of 2-furoic acid (9.6 mM) in MeOH was passed continuously through a fluid-bed reactor using a Jasco HPLC pump at a rate of 0.100 mL/min. The reactor was a 5 mL Onmifit® column, where the corresponding photocatalyst was swelled and suspended under stirring. The reactor used a medium-pressure Hg lamp (lamp power 75%, approximately 112.5 W), and all the required connections were made with FEP coil. A quartz glass was used as filter. The flow stream was passed through an 8-bar back pressure valve. The reaction stream of crude product was collected into a round-bottom flask, and the samples taken analyzed by UV-Visible to determine the conversion and yield.

Acknowledgements

This research work was supported by the Spanish MINECO (RTI2018-098233-B-C22) and Generalitat Valenciana (PROMETEO/ 2016/071). D. V. thanks UNED (Costa Rica) for a predoctoral fellowship. The technical support of the SCIC at the Universitat Jaume I is acknowledged.

Keywords: photocatalysis • Ionic Liquids • Supported Ionic Liquids • Rose Bengal • Flow Chemistry

[1] A. A. Ghogare, A. Greer, *Chem. Rev.* **2016**, *116*, 9994-10034.
[2] A. Albini, M. Fagnoni, *Green Chem.* **2004**, *6*, 1-6
[3] I. Pibiri, S. Buscemi, A. P. Piccionello, A. Pace, ChemPhotoChem **2018**, *2*, 535-547.
[4] J. Wahlen, D. E. De Vos, P. A. Jacobs, P. L. Alsters, *Adv. Synth. Catal*. **2004**, *346*, 152-164.
[5] D. Friedmann, A. Hakki, H. Kim, W. Choi, D.Bahnemann, *Green Chem*. **2016**, *18*, 5391-5411.
[6] Z. Xie, C. Wang, K. E. deKrafft, W. Lin, *J. Am. Chem. Soc.* **2011**, *133*, 2056-2059.
[7] S. Lacombe, T. Pigota, *Catal. Sci. Technol*. **2016**, *6*, 1571-1592.
[8] L. Petrizza, M. Le Bechec, E. Decompte, H. El Hadri, S. Lacombe, M. Save, *Polym. Chem*. **2019**, Advance Article, 10.1039/C9PY00157C.
[9] a) B. Altava, M. I. Burguete, E. García-Verdugo, S. V. Luis, *Chem. Soc. Rev*. **2018**, *47*, 2722-2771. b) B. Altava, M. I. Burguete, E. García-Verdugo, S. V. Luis, M. J. Vicent, J. A. Mayoral, *React. Funct. Polym.* **2001**, *48*, 25-35.
[10] J. Paczkowski, D. C. Neckers, *Macromolecules* **1985**, *186*, 1245-1253.
[11] M. Suzuki, Y. Ohta, H. Nagae, T. Ichinohe, M. Kimura, K. Hanabusa, H. Shirai, D. Wohrle, *Chem. Commun*. **2000**, 213-214.
[12] J. P. Hallett, T. Welton, *Chem. Rev*. **2011**, *111*, 3508-3576.
[13] T. Welton, *Biophysical Rev*. **2018**, *10*, 691-706.
[14] Y. Qiao, W. Ma, N. Theyssen, C. Chen, Z. Hou, *Chem. Rev*. **2017**, *117*, 6881-6928.
[15] M. I. Qadir, M. Zanatta, E. S. Gil, H. K. Stassen, P. Gonçalves, B. A. D. Neto, P. E. N. De Souza, J. Dupont, *ChemSusChem* **2019**, *12*, 1011-1016.
[16] B. Murphy, P. Goodrich, C. Hardacre, M. Oelgemöller, *Green Chem*. **2009**, *11*, 1867-1870.
[17] H. Garcia, S. Navalon, *RSC Cat. Series* **2014**, *15*, 474-507.
[18] H. Shimakoshi, N. Houfuku, L. Chen, Y. Hisaeda, Y. *Green Energy and Env*. **2019**, Article in Press.
[19] D. C. Fabry, M. A. Ronge, M. Rueping, *Chem. Eur. J*. **2015**, *21*, 5350-5354.
[20] W. Zhang, H. Shimakoshi, N. Houfuku, X.-M. Song, Y. Hisaeda, *Dalton Trans.* **2014**, *43*, 13972-13978.
[21] D. Xu, H. Zhang, X. Chen, F. Yan, *J. Mat. Chem. A* **2013**, *1*, 11933-11941.
[22] A. Rosspeintner, M. Koch, G. Angulo, E. Vauthey, E. *J. Phys. Chem. Letters* **2018**, *94*, 7015-7020.
[23] A. Aster, E. Vauthey, *J. Phys. Chem. B* **2018**, *122*, 2646-2654.
[24] F. Giacalone, M. Gruttadauria, *ChemCatChem* **2016**, *8*, 664-684.
[25] a) M. I. Burguete, F. Galindo, E. García-Verdugo, N. Karbass, S. V. Luis, *Chem. Commun.* **2007**, 3086-3088. b) V. Sans, N. Karbass, M. I. Burguete, V. Compañ, E. García-Verdugo, S. V. Luis, M. Pawlak, *Chem. Eur. J*. **2011**, 17, 1894-1906.
[26] R. Porcar, B. Altava, E. Verdugo, S. V. Luis in Green Synthetic Processes and Procedures, (Ed. R. Ballini), Green Chemistry Series, RSC, Cambridge, **2019**, pp. 289-318.
[27] E. García-Verdugo, B. Altava, M. I. Burguete, P. Lozano, S. V. Luis, *Green Chem.* **2015**,*17*, 2693-2713.
[28] D. Mecerreyes, *Progr. Polym. Sci.* **2011**, *36*, 1629-1648.
[29] E. Andrzejewska, *Polym. Int.* **2017**, *66*, 366-381.
[30] W. Qian, J. Texter, F. Yan, *Chem. Soc. Rev.* **2017**, *46*, 1124-1159.

[31] P. Lozano, E. García-Verdugo, R. Piamtongkam, N. Karbass, T. De Diego, M. I. Burguete, S. V. Luis, J. L. Iborra; *Adv. Synth. Catal*. **2007**, *349*, 1077-1084.

[32] G. Vassilikogiannakis, M. Stratakis, *Angew. Chem., Int. Ed.* **2003**, *42*, 5465-5468.

[33] G. I. Ioannou, T. Montagnon, D. Kalaitzakis, S. A. Pergantis, G. Vassilikogiannakis, *Org. Biomol. Chem.* **2017,** *15*, 10151-10155.

[34] S. Martín, R. Porcar, E. Peris, M. I. Burguete, E. García-Verdugo, S. V. Luis, *Green Chem.* **2014**,*16*, 1639-1647.

[35] R. Porcar, P. Lozano, M. I. Burguete, E. Garcia-Verdugo, S. V. Luis, *React. Chem. Eng.* **2018**, *3*, 572-578.

[36] J. Restrepo, R. Porcar, P. Lozano, M. I. Burguete, E. García-Verdugo, S. V. Luis, *ACS Catal.* **2015**, *5*, 4743-4750.

[37] D. C. Neckers, J. Paczkowski, *J. Am. Chem. Soc.* **1986**, *108*, 291-292.

[38] M. Nowakowska, M. Kepczyński, M. Dabrowska, *Macromol. Chem. Phys.* **2001**, *202*, 1679-1688.

[39] O. Valdes-Aguilera, D. C. Neckers, *J. Phys. Chem*. **1988**, *92* , 4286-4289.

[40] N. Hildebrandt, C. M. Spillmann, W. R. Algar, T. Pons, M. H. Stewart, E. Oh, K. Susumu, S. A. Dıaz, J. B. Delehanty, I. L. Medintz, *Chem. Rev*. **2017**, *117*, 536-711.

[41] V. Fabregat, M. I. Burguete, S. V. Luis, F. Galindo, *RSC Adv*. **2017**, *7*, 35154-35158.

[42] D. Cambié, C. Bottecchia, N. J. W. Straathof, V. Hessel. T. Noël, *Chem. Rev.* **2016**, *116*, 10276–10341.

[43] J. Tang, H. Tang, W. Sun, M. Radosz, Y. Shen, *J. Polym. Sci., Part A: Polym. Chem*. **2005**, *43*, 5477-5489.

[44] M. I. Burguete, E. Garcıa-Verdugo, S. V. Luis, J. A. Restrepo, *Phys. Chem. Chem. Phys*. **2011**, *13*, 14831-14838.

[45] B. Altava, M. I. Burguete, F. Galindo, R. Gavara, S.V. Luis, *J. Comb. Chem.*, **2004**, *6*, 859-861.

[46] M. I. Burguete, F. Galindo, R. Gavara, S. V. Luis, M. Moreno, P. Thomas, D. A. Russell, *Photochem. Photobiol. Sci.*, **2009**, 8, 37-44.

[47] W. Fudickar, T. Linker, *Chem. Commun.*, **2008**, 1771-1773.

Entry for the Table of Contents

FULL PAPER

Polymers containing imidazolium units are excellent and tunable supports enhancing the stability and activity of Rose Bengal as photooxidation catalyst under batch and flow conditions.

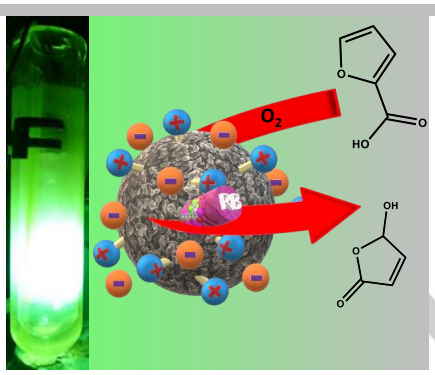

David Valverde, Raul Porcar, Diana Izquierdo, M. Isabel Burguete, Eduardo Garcia-Verdugo and Santiago V. Luis**

Page No. – Page No.

Rose Bengal immobilized onto Supported Ionic Liquid-like Phases: Efficient photocatalyst for batch and flow processes